Simulation and Comparison of the Run Length of an Ethane Cracking Furnace with Reactor Tubes of Circular and Elliptical Cross Sections

ARTICLE *in* INDUSTRIAL & ENGINEERING CHEMISTRY RESEARCH · JANUARY 1998

Impact Factor: 2.59 · DOI: 10.1021/ie970184z

2 AUTHORS:

Geraldine J. Heynderickx
Ghent University
98 PUBLICATIONS **983** CITATIONS

SEE PROFILE

Gilbert F. Froment
Texas A&M University
85 PUBLICATIONS **4,100** CITATIONS

SEE PROFILE

Article

Simulation and Comparison of the Run Length of an Ethane Cracking Furnace with Reactor Tubes of Circular and Elliptical Cross Sections

Geraldine J. Heynderickx, and Gilbert F. Froment

Ind. Eng. Chem. Res., **1998**, 37 (3), 914-922 • DOI: 10.1021/ie970184z

Simulation and Comparison of the Run Length of an Ethane Cracking Furnace with Reactor Tubes of Circular and Elliptical Cross Sections

Geraldine J. Heynderickx* and Gilbert F. Froment

Laboratorium voor Petrochemische Techniek, Universiteit Gent, Krijgslaan 281, B9000 Gent, Belgium

The on-stream time of cracking furnaces is limited by the formation of coke on the internal skin of the reactor tubes. Rigorous simulations of an ethane cracking furnace, coupling reactor and furnace models with the kinetics of coke formation, prove that the run length of the furnace can be augmented by more than 40% by replacing the cracking tubes of circular cross section by cracking tubes of elliptical cross section. The increase of furnace heat-transfer efficiency and the more uniform circumferential heat fluxes and temperatures favor the run length of the furnace with tubes of elliptical cross section.

Introduction

Thermal cracking of hydrocarbons to olefins is an endothermal process accompanied by the formation of coke on the inner surface of the cracking coils suspended in a pyrolysis furnace. Fouling of the cracking coils has major consequences on the operation of the furnace. First of all, the coke layer reduces the heat transfer from the furnace to the process gas, since coke is a very poor heat conductor. If the feed conversion is to be maintained, a higher heat input to the furnace is required, resulting in a rise of the external tube skin temperature and a decrease of the thermal efficiency of the furnace. The tube skin temperature, gradually increasing in time, reaches a maximum value imposed by the tube metallurgy. The cracking run has to be stopped to decoke the reactor tubes by controlled combustion of the coke layer with a steam/air mixture. Second, the growing coke layer on the internal tube skin reduces the cross section of the reactor tube. With a constant feed rate to the reactor coil, the pressure drop over the reactor tube increases. Since the process gas outlet pressure is normally imposed, the feed inlet pressure increases during the run length of the furnace, and this is detrimental for the ethylene selectivity. Too high an inlet pressure can also cause the cracking run to be stopped for decoking the tubes. Reactor geometry, operating conditions, and feedstock composition determine which of the two described effects causes the production cycle to be stopped.

Decoking of the reactor tubes involves a significant loss in production capacity and should be limited to a minimum. This can only be obtained by reducing the rate of coke formation. The coking rate is determined by the interface temperature between the process gas and the coke layer (Sundaram and Froment, 1979). Limiting the interface temperature results in lower coking rates and a longer run length of the furnace.

Simulation results have shown that significant circumferential nonuniformities in heat flux, tube skin, and coking rate profiles exist, due to the presence of "front" sides and "shadow" sides on the tubes (Heynderickx and Froment, 1996). It was also shown that circumferential coking rates can be reduced up to 30% by replacing cylindrical tubes by tubes with an elliptical cross section.

The present paper presents the results of run length simulations of an ethane cracking furnace with cracking tubes of circular and elliptical cross sections. Higher heat-exchanging efficiencies and/or more uniform circumferential temperature distributions and coke layers in the tubes of elliptical cross section favor the run length of the furnace with elliptical tubes. The run length simulations provide detailed information on the coking process, so that the operating conditions and the cracking results can be evaluated over the total run length of the cracking furnace.

Model Equations and Simulation Procedure

Reactor Model. The set of continuity equations for the various species is solved simultaneously with the energy equation and the pressure drop equation (Froment and Bischoff, 1990):

$$\frac{\mathrm{d}F_j}{\mathrm{d}z} = (\sum_i n_{ij} r_{ri}) \frac{\pi d_t^2}{4} \tag{1}$$

$$\sum_j F_j c_{pj} \frac{\mathrm{d}T}{\mathrm{d}z} = Q(z)\pi d_t + \frac{\pi d_t^2}{4} \sum_i r_{ri}(-\Delta H)_i \tag{2}$$

$$\left(\frac{1}{M_m p_t} - \frac{p_t}{\alpha G^2 R T}\right) \frac{\mathrm{d}p_t}{\mathrm{d}z} = \frac{d}{\mathrm{d}z}\left(\frac{1}{M_m}\right) + \frac{1}{M_m}\left(\frac{1}{T}\frac{\mathrm{d}T}{\mathrm{d}z} + Fr\right) \tag{3}$$

with the friction factor (Knutzen and Katz, 1958)

$$Fr = 0.092 \frac{Re^{-0.2}}{d_t} \tag{4}$$

for the straight parts of the reactor coils and

$$Fr = 0.092 \frac{Re^{-0.2}}{d_t} + \frac{\zeta}{\pi R_b} \tag{5}$$

* Author to whom correspondence is addressed. E-mail: gh@elptrs1.rug.ac.be.

S0888-5885(97)00184-X CCC: $15.00
Published on Web 01/22/1998

for the tube bends, with (Nekrasov, 1969)

$$\zeta = \left(0.7 + 0.35\frac{\Lambda}{90°}\right)\left(0.051 + 0.19\frac{d_t}{R_b}\right) \qquad (6)$$

For the tubes of elliptical cross section, the tube diameter d_t is replaced by the equivalent (hydraulic) tube diameter d_e:

$$d_e = 4\frac{S}{O} \qquad (7)$$

A detailed radical reaction scheme is combined with a one-dimensional plug-flow model to simulate the cracking reactions in the reactor coil. Reynolds numbers on the order of 250 000 are calculated in the reactor tubes. The turbulence wipes out temperature profiles in the process gas over the cross section of the reactor tubes.

The kinetic scheme is based on a complete reaction network for the decomposition of the ethane feed. The CRACKSIM reaction network contains 1054 reactions: 56 initiation reactions, 572 H-abstractions, 126 radical additions, 126 decomposition reactions, 6 isomerization reactions, 56 termination reactions, and a number of molecular Diels−Alder cyclizations (Sundaram and Froment, 1978; Willems and Froment, 1988a,b).

Coke formation at any time during the cracking run and at any position in the reactor tube is calculated from the continuity equation (Plehiers et al., 1990):

$$\frac{\partial C_C}{\partial t} = R_C \qquad (8)$$

Rate expressions R_C for the coke formation in the thermal cracking of ethane and propane have been derived by Sundaram and Froment (1979) and Sundaram et al. (1981). A number of coke precursors were found to contribute to the formation of coke:

$$R_C = \sum_i r_{C,i} \qquad (9)$$

Furnace Model. The furnace model is based upon the zone method of Hottel and Sarofim (1967). The furnace wall, the tube skin, and the flue gas volume are divided into a number of isothermal elements with uniform properties. For each of these elements, named zones, the energy balance is set up, taking into account the contributions of convective, conductive, and radiative heat transfer. The contributions of radiative transfer are obtained through Monte Carlo simulation (Plehiers and Froment, 1989), calculating the view factors between the different zones in the furnace. From these view factors, the total exchange areas Z_iZ_j between the zones Z_i and Z_j in the furnace are determined. The total exchange area Z_iZ_j is the amount of radiative energy emitted by the zone Z_i in the direction of the zone Z_j, divided by the blackbody emissive power of the zone Z_i. The emissive power of a blackbody with temperature T_i is calculated from the Stefan−Boltzmann law:

$$E_i = \sigma T_i^4 \qquad (10)$$

The determination of Z_iZ_j is discussed in detail by Rao et al. (1988) and by Plehiers and Froment (1989).

The set of energy balances for the furnace can be written as

$$\begin{bmatrix} Z_1Z_1 - \sum_j Z_1Z_j & Z_2Z_1 & \dots & Z_nZ_1 \\ Z_1Z_2 & Z_2Z_2 - \sum_j Z_2Z_j & \dots & Z_nZ_2 \\ \vdots & \vdots & \vdots & \vdots \\ Z_1Z_n & Z_2Z_n & \dots & Z_nZ_n - \sum_j Z_nZ_j \end{bmatrix} \times \begin{bmatrix} E_1 \\ E_2 \\ \vdots \\ E_n \end{bmatrix} = \begin{bmatrix} Q_1A_1 \\ Q_2A_2 \\ \vdots \\ Q_nA_n \end{bmatrix} \qquad (11)$$

where Q_i represents the nonradiative heat flux emitted by the zone Z_i with area A_i.

Solving this set of energy equations yields the heat flux and temperature profiles in the furnace. To calculate the circumferential temperature distribution in the tube wall, the tubes are discretized along the tube perimeter and over the tube skin. By constructing and solving the energy balance for each element in the tube skin, circumferential heat flux and temperature profiles are calculated in the tube skin. The form of these energy balances for the zones in the tube skin is discussed by Heynderickx et al. (1992). They are obtained by discretizing the conduction equation for each zone in the reactor tube skin, accounting for the appropriate boundary conditions:

$$\nabla^2 T = \frac{d^2T}{dr^2} + \frac{1}{r} + \frac{dT}{dr} + \frac{1}{r^2} = 0 \qquad (12)$$

$$\lambda \nabla T(\theta,r) = q(\theta,r) \qquad r = r_{ext}; \quad \forall\theta$$

$$\lambda \nabla T(\theta,r) = h_p(T(\theta,r) - T_p) \qquad r = r_{int}; \quad \forall\theta$$

Simulation Procedure

A simplified flowchart of the iterative calculation scheme is given in Figure 1. Predicting the run length of the cracking furnace requires the simultaneous solution of the set of differential and algebraic equations (1)−(3), (8), (11), and (12). By assuming an incremental pseudo steady state for the cracking reactions (coking reactions are much slower than cracking reactions), the run time of the cracking furnace can be augmented in a stepwise manner (outer loop in Figure 1). For each time increment a coupled furnace and reactor simulation has to be performed by simultaneously solving the set of equations (1)−(3), (11), and (12). For that purpose, a double iterative scheme is used. Starting from initial estimates for temperatures and fluxes, the energy balances (11) are constructed and solved. This provides better estimates for the zone temperatures. From the tube skin and process gas temperatures, new flux estimates are calculated. Based on these new fluxes, the process gas composition, temperature, and pressure are calculated from equations (1)−(3). By solving (12), new zone temperatures are obtained which are compared to the previously obtained values. The cycle is repeated until convergence is reached for the time increment. Time increments of 60 h of furnace run time were found to be sufficiently small to justify pseudo

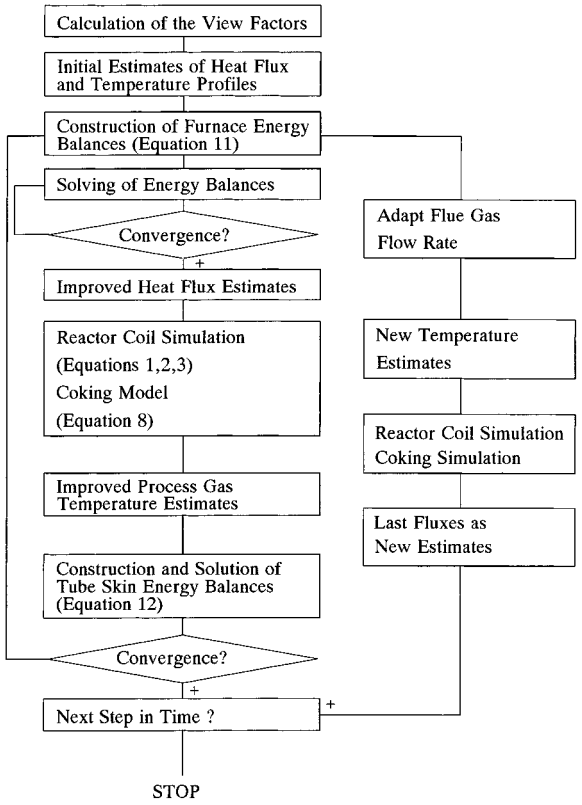

Figure 1. Flow diagram of the calculations.

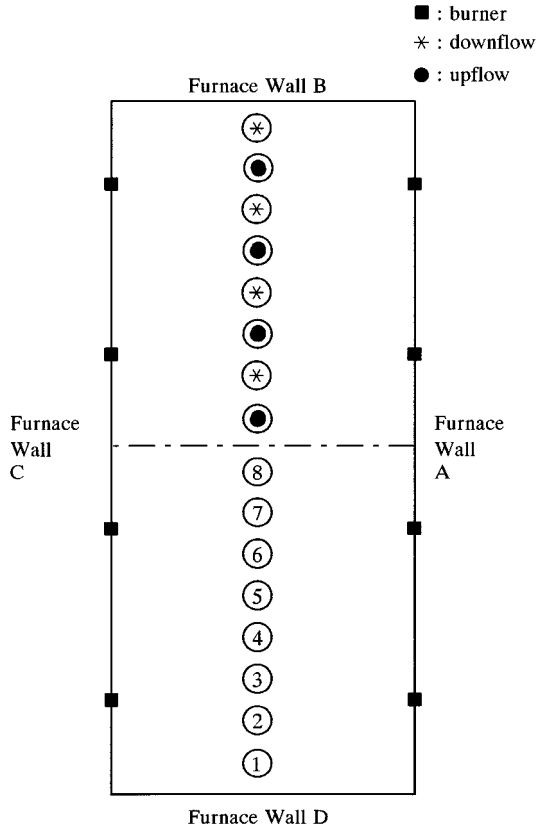

Figure 2. Top view of the ethane furnace.

steady state. A total of 20−28 time steps were taken for each of the three run length simulations that have been performed. The three run length simulations reported here each required around 8 h of CPU time on an IBM/RS6000/375 computer.

For each run length simulation, the crossover temperature of the process gas was kept constant at a value of 600 °C. However, the process gas inlet temperature is determined by the heat transfer in the convection section of the furnace, and thus by the flue gas outlet temperature in the radiation section of the furnace. The flue gas outlet temperature differs for both coil types and rises with time. Accounting for these variations in crossover temperature requires the calculation of the convection section of the furnace and would introduce an additional iteration loop in the calculations. Simulation time would be augmented by a factor of 2, without adding meaningful precision to the calculation results.

Furnace Description

The main dimensions and operating conditions of the ethane cracking furnace are summarized in Table 1.

Two reactor coils, with 8 passes each, are suspended in the furnace which is heated by means of 64 radiation burners positioned in 8 rows of 4 burners in the front and in the rear wall of the furnace. A top and front view of the furnace are shown in Figures 2 and 3.

The internal cross section of the elliptical tubes was taken to be equal to that of the circular tube, allowing for hydrocarbon feed and steam rates identical for the reactor coils of both types, and thus for identical furnace capacity. The process gas pressure drop in both tube types can easily be compared (eq 3). The external major axis of the elliptical tube was taken to exceed the external diameter of the circular tube by 40%. Based on the results of Heynderickx and Froment (1996),

Table 1. Furnace Dimensions and Operating Conditions

		elliptical	
	circular	long	short
Furnace			
length (mm)	4652	4652	4652
height (mm)	13450	13450	12400
width (mm)	2100	2100	2100
thickness of refactory (mm)	230	230	230
thickness of insulation (mm)	50	50	50
no. of side wall burners	64	64	64
Firing Conditions			
initial total heat input (MW)	14.00	13.65	14.16
final total heat input (MW)	14.43	14.00	14.61
Operating Conditions			
feedstock	100% ethane		
hydrocarbon feed rate	3500 kg/h/coil		
steam dilution	0.350 kg/kg		
coil inlet temperature	600 °C		
coil outlet pressure	1.622 atm		
Material Properties			
emisivity of furnace wall	0.60		
emissivity of tube skin	0.95		
thermal conductivity of			
refractory (W/m·K)	$0.0193 + 118.0 \times 10^{-6}T$ (K) (at 1373 K: 0.18 W/m·K)		
insulation (W/m·K)	$0.0452 + 111.1 \times 10^{-6}T$ (K)		
tube skin material (W/m·K)	$-8.432 + 3.040 \times 10^{-2}T$ (K) (at 750 °C: 22.67 W/m·K) (at 1050 °C: 31.79 W/m·K)		
coke (W/m·K)	6.46		

simulation results for elliptical tubes of lower eccentricity can be expected to vary between the simulation results presented for circular and elliptical tubes in this paper. The dimensions of both tube types are compared in Table 2. The perimeters of the elliptical tubes were determined by numerical integration of the elliptical integral of the second kind:

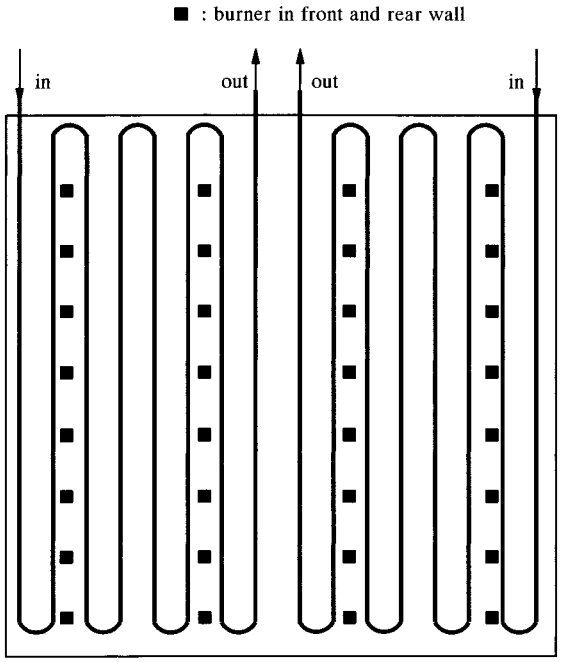

Figure 3. Front view of the ethane furnace.

Table 2. Tube Dimensions

		elliptical	
tube type	circular	long	short
external major axis/diameter	1.0	1.4	1.4
eccentricity ϵ	0	0.86	0.86
total coil length (m)	102.336	102.336	93.976
no. of passes	8	8	8
internal cross section			
passes 1−6 (m^2)	0.012076	0.012076	0.012076
passes 7 and 8 (m^2)	0.014527	0.014527	0.014527
wall thickness (mm)	8	8	8
external diameter (mm)			
passes 1−6	140		
passes 7 and 8	152		
external major axis (mm)			
passes 1−6		196	196
passes 7 and 8		212.8	212.8
external minor axis (mm)			
passes 1−6		101.42	101.42
passes 7 and 8		109.98	109.98
external perimeter (mm)			
passes 1−6	439.8	479.1	479.1
passes 7 and 8	477.5	520.0	520.0

$$P = 4a\int_0^{\pi/2}\sqrt{1-\left(1-\frac{b^2}{a^2}\right)\sin^2\phi}\,\mathrm{d}\phi \qquad (13)$$

In this expression, ϕ represents the angle of the parameter equation of the ellipse (Figure 4)

$$x = a\sin\phi \qquad \text{and} \qquad y = b\cos\phi \qquad (14)$$

with a and b the semimajor and semiminor axes of the ellipse.

For identical cross sections of both tube types, the perimeter of the elliptical tube exceeds that of the circular tube by 9%. Since the surface-to-volume ratio of the elliptical tube is larger, this results in higher friction losses for the process gas. Two run length simulations for furnaces with elliptical tubes were performed. For the first simulation the coil length was taken equal to that of the coil with circular tubes. This results in a 9% rise of the total heat-exchanging surface. For the second simulation, the length of the coil with

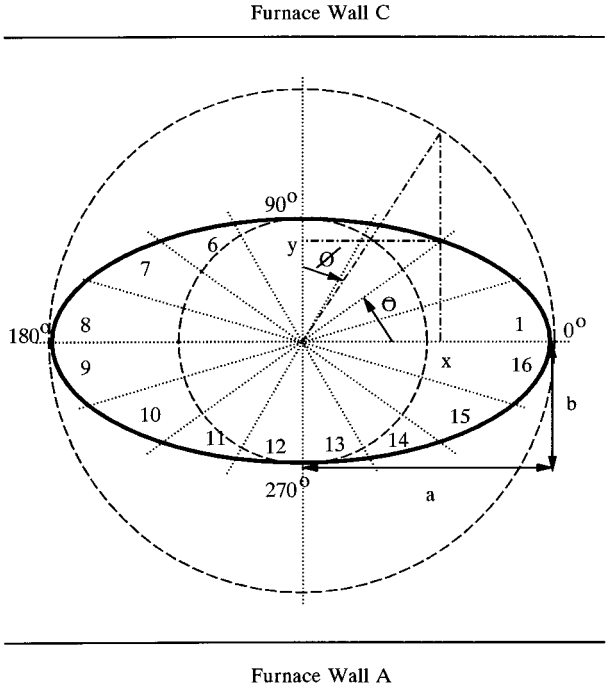

Figure 4. Circumferential division of the tube.

elliptical tubes was reduced to obtain a total heat-exchanging surface equal to that of the coil with circular tubes. The center-to-center distance (pitch) between the tubes was the same for both tube types in order to retain the furnace length. For the elliptical coil of reduced length, the furnace height is reduced by 1 m. This implies an 8% reduction of the furnace volume. The furnace was divided into zones by means of four planes parallel to the furnace bottom plate. The five axial zones on the fourth, fifth, and sixth pass of the reactor coil through the furnace were circumferentially divided into 16 zones of equal area, as presented in Figure 4 for the tube with elliptical cross section.

Accounting for symmetry in the furnace, a total of 162 zones are obtained: 145 (external) tube skin zones, 12 furnace wall zones, and 5 flue gas volume zones.

Results and Discussion

The operating policy of the ethane cracking furnace consisted of keeping the ethane conversion at the outlet of the cracking coil at a constant level of 57.65% during the whole run, for the three coils. A constant outlet conversion requires a constant total heat input to the process gas. Due to the formation of coke, a poor heat conductor compared to the tube skin material (Table 1), the external tube skin temperature rises with run time. To achieve the constant outlet conversion under these conditions, the heat input to the furnace must increase with time, as shown in Figure 5. For the furnace with the coil of circular cross section, the heat input rises by 3.1% from an initial value of 14 MW to a final value of 14.43 MW; for the furnace with the longer coil of elliptical cross section, the respective values are 13.65 MW and 13.995 MW, a rise of 2.5%; for the furnace with the shorter coil of elliptical cross section, a 3.2% rise from an initial 14.16 MW to a final 14.61 MW is calculated. Consequently, the flue gas outlet temperature rises (Figure 5); an increase of 36 °C is calculated for each of the three furnaces. The firing duty of the furnace with the longer elliptical coil is 2.5% lower than

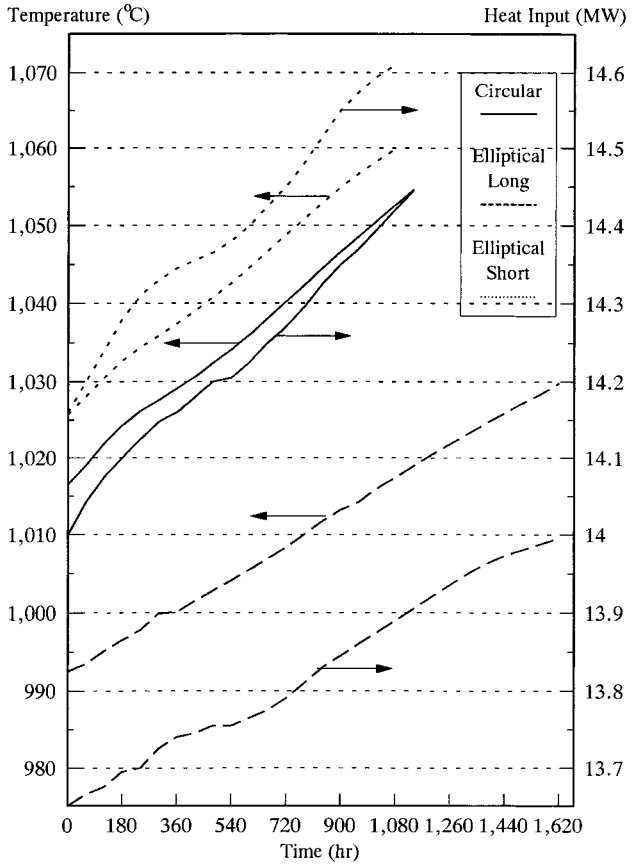

Figure 5. Furnace heat input and flue gas outlet temperature as a function of time.

that of the furnace with the circular coil. This is mainly due to the 9% rise of the heat-exchanging surface which strongly affects the thermal efficiency of the furnace. The thermal efficiency varies between 51.25% and 49.25% during the run length of the furnace with the longer elliptical coil, while values between 49.97% and 47.94% are calculated for the furnace with the circular coil. Reducing the length of the coil by 8% inevitably results in a drop of the thermal efficiency of the furnace: values between 49.56% and 47.75% are calculated for the furnace with the shorter elliptical coil. As a result a 1% higher heat input is required.

During the calculations, the process gas outlet pressure was kept constant at a value of 1.622 atm, the value used in the industrial practice of the calculated furnace. Due to the formation of a coke layer on the internal tube skin, the internal cross section of the tubes decreases, resulting in a higher pressure drop over the reactor. To maintain the required outlet pressure, the inlet pressure has to increase with time. The inlet pressure for the longer coil with tubes of elliptical cross section grows slower than that for the tubes with circular section, due to the lower rate of coke formation and the corresponding thinner coke layer. For the shorter elliptical coil, the difference with the circular coil is minor. For the reactor coil with circular cross section, the process gas inlet pressure is 3.2 atm at the start of the run and 3.76 atm at the end of the run; for the longer cracking coil with tubes of elliptical cross section, the respective values are 3.264 and 4.17 atm; for the shorter coil, values of 3.17 and 3.75 atm are calculated. The total pressure drop over the reactor coil is rather low, which is typical for a swaged coil with large diameter (Figure 6a,b). The pressure drop in the seven bends of the coils amounts to 30% of the total pressure drop. The largest pressure drop contribution is encountered in the last two bends of the reactor coil, where coke layers are thick. The higher inlet pressure for the longer elliptical coil requires a higher compression energy for the process gas. This additional compression energy is negligible when compared with the gain in furnace heat input. Furthermore, a scrutiny of Figure 6b shows that the process gas pressure profiles for the shorter elliptical tube are "horizontally compressed" copies of the profiles for the circular tubes. Since this is found for all profiles (heat flux, temperature, coking rate, ...), no further profiles for the shorter elliptical tubes are shown.

As already mentioned, the rise of process gas pressure is detrimental for the ethylene selectivity (Figure 7), while the formation of methane and benzene, for example, are favored by higher pressure values (Plehiers et al., 1990). The relative loss in ethylene production due to the use of the longer elliptical coil is less than 0.1%. Furthermore, if firing costs are supposed to be 15% of the ethylene production cost, the ethylene produced in the longer elliptical coil costs 0.5% less than the ethylene from the circular tubes.

Figure 8 shows the axial external heat flux profiles. The peaks correspond to the bottom bends of the coils and the valleys to the top bends. With growing run time of the furnace, the heat input in the first part of the coil, where coking rates are low due to low temperatures, increases. The heat input in the last part of the coil, where thick coke layers form an additional resistance to heat transfer, decreases. This also explains why the process gas temperature profiles grow more convex with time.

The axial coking rate profiles are presented in Figure 9. In the first part of the coil, the coking rates increase with time, due to the rising process gas/coke layer interface temperatures, resulting from higher local heat fluxes (Figure 8). In the last part of the coil, the opposite effect is observed. The coking rate reaches a maximum value in the last U-bend of the coil, where temperatures reach a maximum value. From Figure 9 it is clear that the coking rates are considerably lower in the furnace with the longer elliptical tubes. Coking rate differences between the coil with circular tubes and the shorter coil with elliptical tubes are found to be negligible.

The evolution of the coke layer thickness is shown in Figure 10. When the furnace is stopped for decoking, maximum coke layer thicknesses of 11.4, 13.6, and 11.2 mm are calculated for the circular, longer elliptical, and shorter elliptical coils, respectively.

As already mentioned, the furnace has to be stopped for decoking when the external tube skin temperature reaches too high a value. A maximum value of 1054.5 °C is imposed by the tube skin metallurgy. The external tube skin temperature profiles are shown in Figure 11. The maximum external tube skin temperature is observed in the last bottom bend of the coil. It rises by 0.093, 0.071, and 0.098 °C/h for the circular, longer elliptical and shorter elliptical coil, respectively. It is calculated that the furnace with circular tubes has to be stopped after a run time of 1160 h (48.3 days); that with the longer elliptical coil after 1670 h (69.5 days); and that with the shorter elliptical, coils after 1100 h (45.8 days). The 44% gain in run time for the furnace with the longer elliptical coil, compared to the furnace

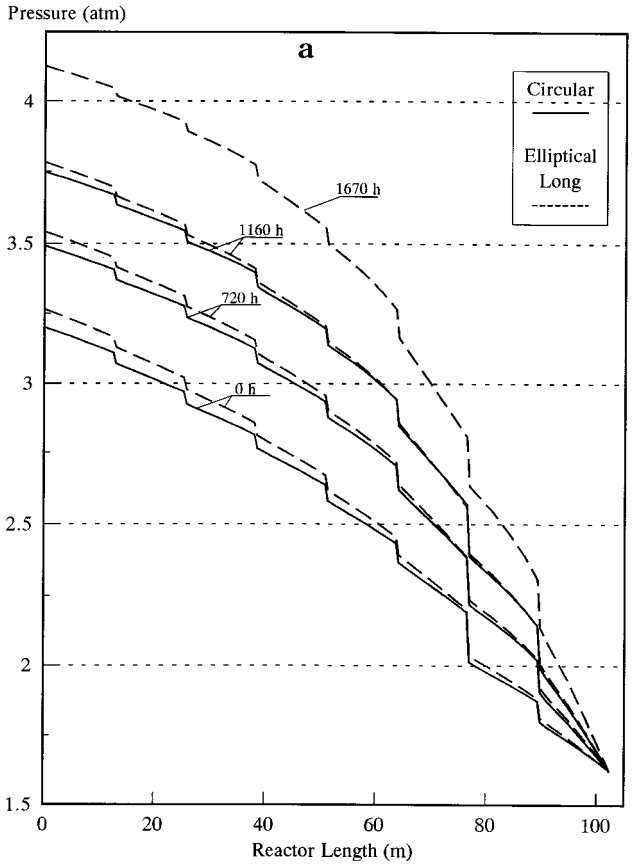

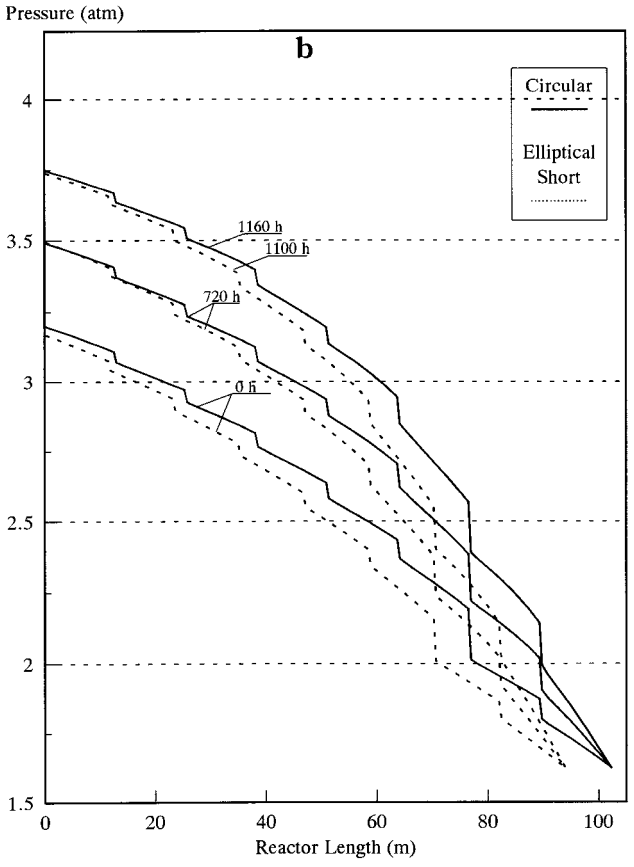

Figure 6. (a and b) Process gas pressure profiles along the coil.

with the circular coil, is mainly due to the higher heat-exchanging surface. This allows lowering of the global temperature level in the furnace without having to change the operating conditions for the reactor coil to retain the conversion level at 57.65%.

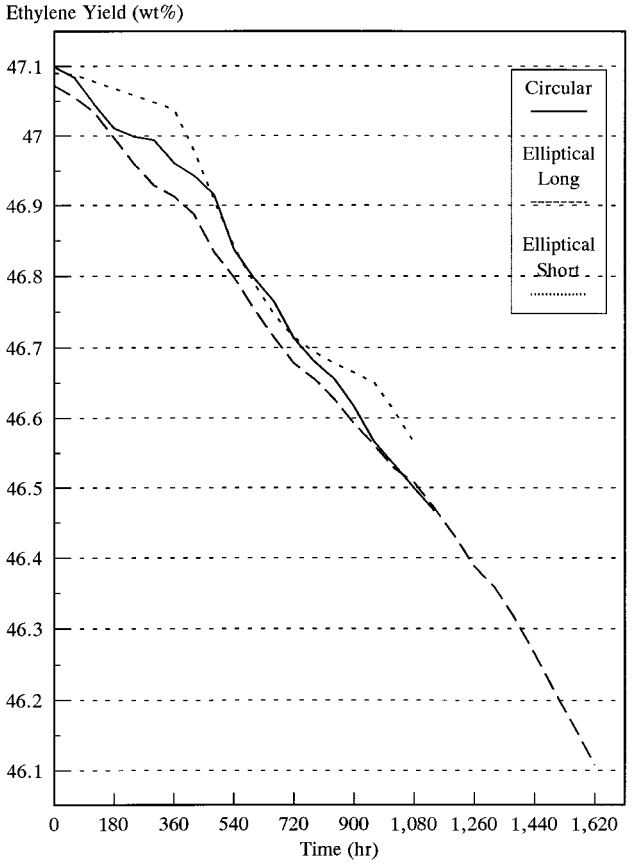

Figure 7. Ethylene yield profiles as a function of time.

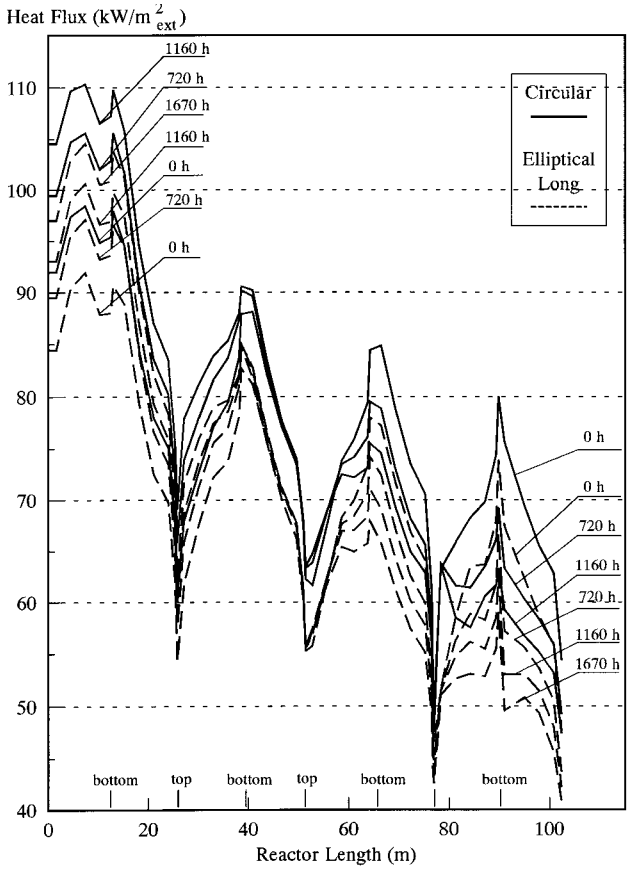

Figure 8. Heat flux profiles along the coil.

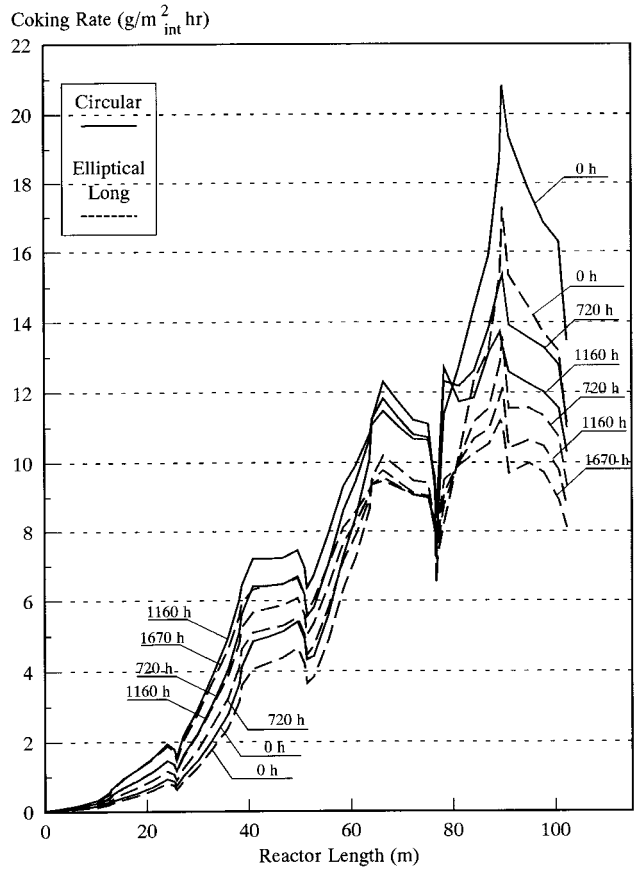

Figure 9. Coking rate profiles along the coil.

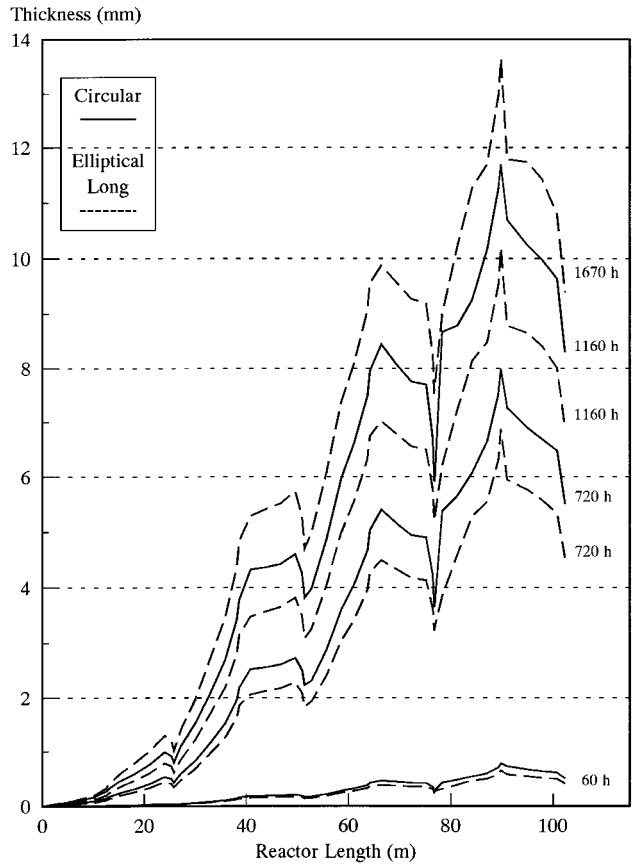

Figure 10. Coke layer thickness profiles along the coil.

Nevertheless, part of the gain in run time is due to the effect of using elliptical tubes. This is proven by the run length simulation for the shorter coil with elliptical cross section. Although the thermal efficiency for the furnace with the shorter elliptical coil drops and, consequently, the global temperature level in the furnace rises to retain the conversion level at 57.65%, the external tube skin temperatures and the run length of the furnace remain practically unchanged, compared to the circular tubes. This is a consequence of the flatter circumferential profiles on the elliptical tubes.

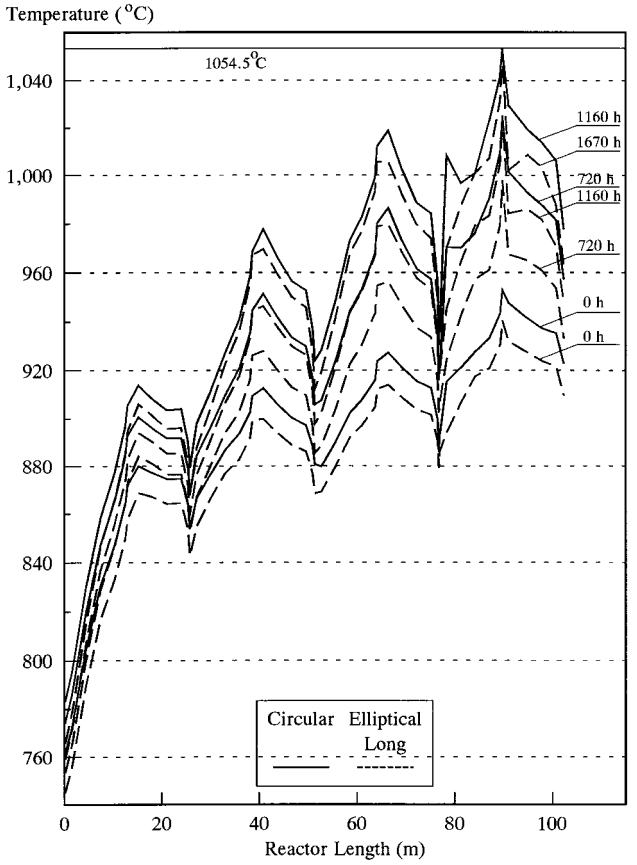

Figure 11. External tube skin temperature profiles along the coil.

Figure 12 presents circumferential heat flux profiles halfway through the fifth pass of the reactor coil. At this position along the coil, heat fluxes already decrease with time (Figure 8) due to thick coke layers on the inner surface of the coil. The circumferential nonuniformities are found to be flattened out with growing run time of the furnace. For the circular tube, at the given position, circumferential nonuniformities in heat flux of 18 and 13 kW/m$^2_{ext}$ are calculated at the start and the end of the run. These values amount to 24% and 17% of the average flux value at the given position. For both elliptical coils, at the same position, circumferential nonuniformities of 8 and 4 kW/m$^2_{ext}$ are calculated, corresponding to 12% and 6% of the average values for the longer coil and to 10% and 5% of the average values for the shorter coil. For the coils of elliptical cross section, heat flux variations around the tube skin are minor. The "front" side of the tube surface, facing the furnace wall and receiving a larger fraction of the furnace wall radiation, is clearly much larger than for the circular tube. Furthermore, the variation *with time* of the heat flux on the circumference of the tubes is concentrated on the front sides of the tubes, where thick coke layers (Figure 13) are formed. Heat flux variations on the shadow sides of the tubes are limited, due to the formation of thinner coke layers. This is also reflected

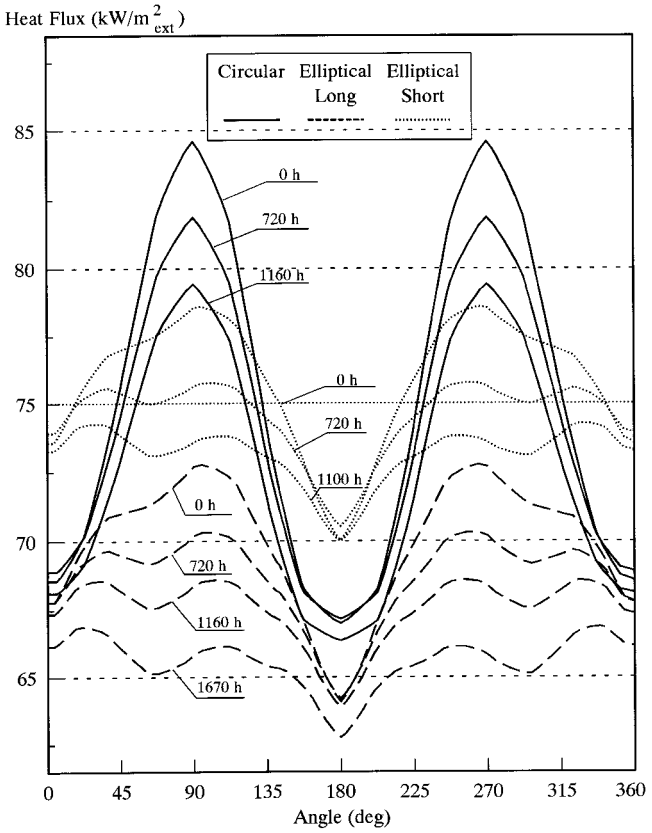

Figure 12. Circumferential external heat flux profiles: tube 5; axial division 3.

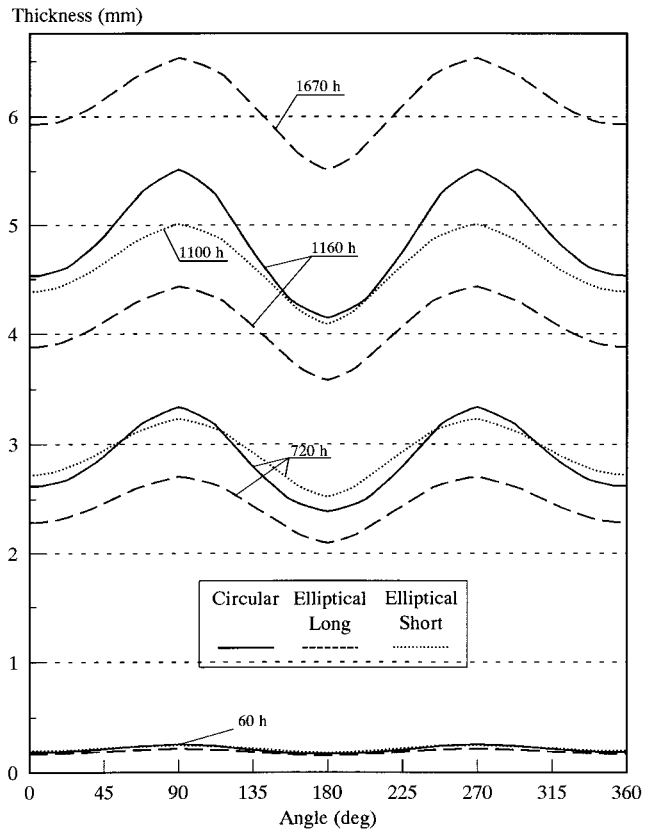

Figure 13. Circumferential coke layer thickness profiles: tube 5; axial division 3.

in the circumferential nonuniformities of the external tube skin temperature (Figure 14). Contrary to the nonuniformities in heat flux, they grow with increasing

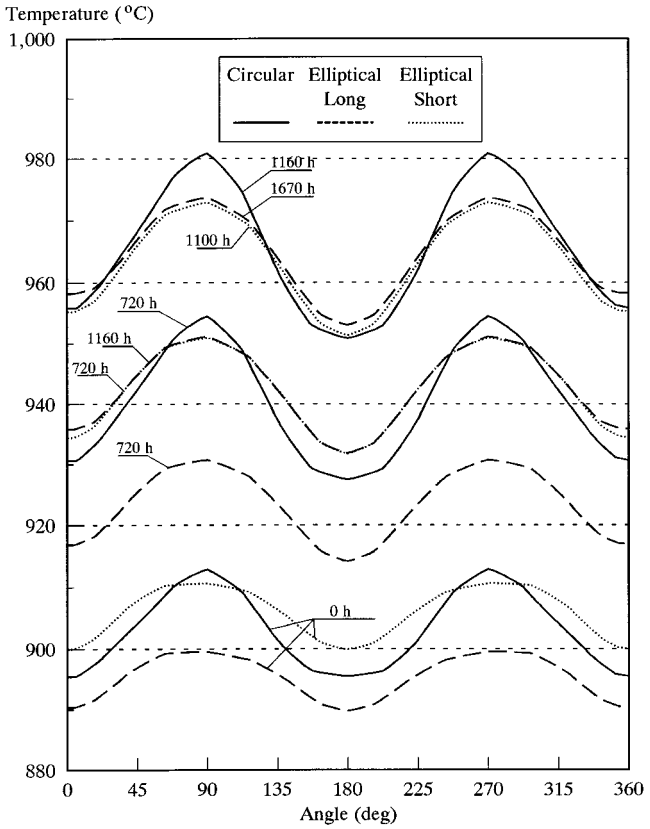

Figure 14. Circumferential external tube skin temperature profiles: tube 5; axial division 3.

run time of the furnace. For the circular tubes, at the given position, the external tube skin temperature varies over 18 °C at the start and 31 °C at the end of the run; an increase of 13 °C over 1160 h (0.0112 °C/h). For the longer elliptical tubes, the corresponding values are 10 and 21 °C, an increase of 11 °C over 1670 h (0.0066 °C/h). For the shorter elliptical tubes, values of 10 and 21 °C are calculated, an increase of 11 °C over 1100 h (0.01 °C/h).

The run length of the industrial furnace with tubes of circular cross section, operating under the given operating conditions is 48 days (1152 h).

Conclusion

The use of thermal cracking coils with tubes of elliptical cross section has a significant beneficial influence on the run length of a thermal cracking furnace due to the higher surface-to-volume ratio of the elliptical tubes and due to the flatter circumferential heat flux, coking rate, and temperature profiles, compared with tubes of circular cross section.

The higher surface-to-volume ratio of the elliptical tubes compared with circular tubes results in a higher thermal efficiency for the furnace. A constant process gas outlet conversion can be obtained with a lower heat input and a lower furnace temperature level than the corresponding values for circular tubes (for coils of equal length). This implies lower tube skin temperatures and a longer run length of the furnace. Run length gains up to 40% can be obtained.

If the temperature level in the furnace with tubes of elliptical cross section is maintained at that of the furnace with tubes of circular cross section, the constant process gas outlet conversion is obtained with a shorter

elliptical coil. Coil length reductions and therefore furnace volume reductions up to 10% are possible.

Nomenclature

A_i: area of zone i (m^2)
a: semimajor axis of the ellipse (m)
b: semiminor axis of the ellipse (m)
C_C: concentration of coke (mol/m^3)
c_p: heat capacity (J/mol·K)
d_e: equivalent (hydraulic) diameter of the elliptical tube (m)
d_t: tube diameter (m)
E: blackbody emissive power (W/m^2)
F: molar flow rate (mol/hr)
G: total mass flux of the process gas (kg/m^2s)
h_p: process gas convection coefficient ($W/m^2·K$)
$-\Delta H$: heat of reaction (J/mol)
M_m: average molecular weight (kg/mol)
n: stoichiometric coefficient
O: wetted perimeter (m)
P: perimeter of the ellipse (m)
p_t: total pressure (Pa)
Q: heat flux (W/m^2)
q: heat flux (W/m^2)
r: radius (m)
$r_{C,i}$: coking reaction rate of precursor i ($mol/m^3·s$)
Re: Reynolds number
R_C: coking reaction rate (mol/m^3s)
R_b: radius of the tube bend (m)
r_r: reaction rate ($mol/m^3·s$)
S: wetted area (m^2)
s: tube pitch (m)
t: time (s)
T: temperature (K)
T_p: process gas temperature (K)
z: axial reactor coordinate (m)
Z_iZ_j: total exchange area between zones i and j (m^2)

Greek Letters

α: unit conversion factor
ϵ: eccentricity of the ellipse
θ: polar coordinates angle (Figure 4) (rad)
ϕ: angle in the parameter equation of the ellipse (Figure 4) (rad)
Λ: tube bend angle (deg)
σ: Stefan−Boltzmann constant (5.7×10^{-8} $W/m^2·K^4$)
λ: tube material conductivity (W/m·K)

Literature Cited

Froment, G. F.; Bischoff, K. B. *Chemical Reactor Analysis and Design*; John Wiley and Sons: New York, 1990.

Heynderickx, G. J.; Froment, G. F. A Pyrolysis Furnace with Reactor Tubes of Elliptical Cross Section. *Ind. Eng. Chem. Res.* **1996**, *35* (7), 2183.

Heynderickx, G. J.; G. Cornelis, G.; Froment, G. F. Circumferential Tube Skin Temperature Profiles in Thermal Cracking Coils. *AIChE J.* **1992**, *38*, 1905.

Hottel, H. C.; Sarofim, A. F. *Radiative Heat Transfer*; McGraw-Hill: New York, 1967.

Knutzen, J. G.; Katz, D. L. *Fluid Dynamics and Heat Transfer*; McGraw-Hill: New York, 1958.

Nekrasov, B. B. *Hydraulics*; Peace Publishers: Moscow, 1969.

Plehiers, P. M.; Froment, G. F. Firebox Simulation of Olefin Units. *Chem. Eng. Commun.* **1989**, *80*, 81.

Plehiers, P. M.; Reyniers, G. C.; Froment, G. F. Simulation of the Run Length of an Ethane Cracking Furnace. *Ind. Eng. Chem. Res.* **1990**, *29*, 636−641.

Rao, M. V. R.; Plehiers, P. M.; Froment, G. F. Simulation of the Run Length of an Ethane Cracking Furnace. *Ind. Eng. Chem. Sci.* **1988**, *43*, 1223.

Sundaram, K. M.; Froment, G. F. Modeling of Thermal Cracking Kinetics. 3. Radical Mechanisms for the Pyrolysis of Simple Paraffins, Olefins and Their Mixtures. *Ind. Eng. Chem. Fundam.* **1978**, *17* (3), 174−182.

Sundaram, K. M.; Froment, G. F. Kinetics of Coke Deposition in the Thermal Cracking of Propane. *Chem. Eng. Sci.* **1979**, *34*, 635−644.

Sundaram, K. M.; Van Damme, P. S.; Froment, G. F. Coke Deposition in the Thermal Cracking of Ethane. *AIChE J.* **1981**, *27*, 946−951.

Willems, P.; Froment, G. F. Kinetic Modeling of the Thermal Cracking of Hydrocarbons, Part 1: Calculation of Frequency Factors. *Ind. Eng. Chem. Res.* **1988a**, *27*, 1959.

Willems, P.; Froment, G. F. Kinetic Modeling of the Thermal Cracking of Hydrocarbons, Part 2: Calculation of Activation Energy. *Ind. Eng. Chem. Res.* **1988b**, *27*, 1966.

Received for review March 3, 1997
Revised manuscript received November 21, 1997
Accepted November 29, 1997

IE970184Z